

Differential Drag as a Means of Spacecraft Formation Control

BALAJI SHANKAR KUMAR

ALFRED NG

Canadian Space Agency

KEISUKE YOSHIHARA

Japan Aerospace Exploration Agency

ANTON DE RUITER, Member, IEEE

Canadian Space Agency

This paper investigates the feasibility of using differential drag as a means of nano-satellite formation control. Differential drag is caused when the ballistic coefficients of the spacecraft in a formation are not equal. The magnitude of differential drag depends on the difference in ballistic coefficients and also the altitude of the spacecraft formation. AGI's Satellite Tool Kit (STK) is used initially to assess the magnitude of drifts caused due to differential drag for different altitudes. This information is then used to show that it is feasible to use differential drag for spacecraft formation control. A simple PID controller is then implemented that adjusts the cross-sectional areas of the satellites such that the energies of the orbits remain equal. Results are presented that show that the control law can maintain the formation separation with reasonable accuracy.

Manuscript received July 19, 2007; revised August 7, 2008 and May 27, 2009; released for publication December 16, 2009.

IEEE Log No. T-AES/47/2/940834.

Refereeing of this contribution was handled by M. Ruggieri.

Authors' addresses: B. S. Kumar, COMDEV Ltd., Cambridge, Ontario N1R 8L2, Canada, E-mail: (skpbalaji@hotmail.com); A. Ng, Spacecraft Engineering, Space Technologies, Canadian Space Agency, Quebec, Canada; K. Yoshihara, Space Technology Demonstration Research Center, Japan Aerospace Exploration Agency, Japan; A. De Ruiter, Carleton University, Ottawa, Canada.

0018-9251/11/\$26.00 © 2011 IEEE

NOMENCLATURE

a	Acceleration, m/s ²
A	Cross-sectional area, m ²
C_d	Drag coefficient
E	Orbital energy, MJ/kg
F10.7	Solar radiation flux index
k_p	Geomagnetic planetary index
K_p	Proportional gain
K_i	Integral gain
K_d	Derivative gain
m	Spacecraft mass, kg
R	Radius vector, km
SFU	Solar Flux Unit, W/m ² Hz
t	Time, seconds
V_{rel}	Velocity relative to the atmosphere, m/s
ω	Angular mean motion, rad/s
ρ	Atmospheric density, kg/m ³
STK	Satellite Tool Kit
HPOP	High-precision orbit propagator

1. INTRODUCTION

The concept of spacecraft formation keeping using drag panels was first proposed by C. L. Leonard [1] in 1989. In her paper, Leonard discussed the feasibility of using differential drag panels as a means of formation keeping of spacecraft formations for low altitude orbits and showed that formation keeping with differential drag is possible. There are many advantages of using differential drag as actuation for formation keeping and they are

- 1) mass savings due to the lack of a conventional propulsion system,
- 2) no contamination from propellant exhaust; ideal for missions that have highly sensitive onboard sensors,
- 3) relative acceleration generated is very small and so there is no shock generated; ideal for missions that have sensors that are very sensitive to shock and vibrations.

However there are also drawbacks of using such a system and they are listed below.

- 1) Cross-track drift is difficult to control.
- 2) Relative positions cannot be controlled to a very high accuracy and in a given frame of time.
- 3) Mathematical modeling of motion is difficult due to numerous unpredictable time-varying factors.

Given the scope and the limitations of the system, the differential drag technology would be ideal for nano-satellite formation flying missions that need coarse control accuracy requirements. Many other propellant-free actuation concepts have been proposed in the literature for nano-satellite formation keeping. They are the Coulomb force concept [2], magnetic dipole interaction concept [3], and

the intracavity photon thruster concept [4]. Most of the above-mentioned concepts require an enormous amount of power and/or work only for extremely small inter-satellite separation distances and none of the above technologies have been validated in space.

Station keeping with differential drag is a proven concept and has been successfully demonstrated by OrbComm [5] for constellation station keeping of their satellites in supplement to propellant-based station keeping. However, there are no missions that have utilized the differential drag concept for spacecraft formation keeping or formation maneuvering.

In the past, there has been an instance when differential drag actually disrupted a spacecraft rendezvous mission. The Snap-1 and Tsinghua were designed by the Surrey Satellite Technology Limited and launched in 2000 aboard a Cosmos-3M rocket. The satellites were placed in orbits of slightly different altitudes. Due to the altitude difference and the different effective cross-sectional areas, the effects of differential drag then dominated the relative dynamics pushing the satellites further and further away. Attempts were initially made by the controllers on ground to reduce the drift by raising the orbit of Snap 1 but the satellites did not come close to each other due to the depletion of onboard fuel.

Differential drag acceleration is caused when there is a difference in one of the following parameters; effective cross-sectional area, mass, drag coefficient, instantaneous altitude (atmospheric density) and the velocity relative to the atmosphere. The acceleration due to aerodynamic drag can be expressed as [6]

$$\bar{a}_{\text{drag}} = -\frac{1}{2} \frac{C_d A}{m} \rho V_{\text{rel}}^2 \frac{\bar{V}_{\text{rel}}}{|V_{\text{rel}}|}. \quad (1)$$

For identical spacecraft flying in a close formation, differential drag acceleration could be achieved by varying the effective cross-sectional area either by changing the spacecraft attitude or by using deployable drag panels. C. L. Leonard [1] in her paper showed that maintaining a formation with drag panels is possible for low altitude orbits (~ 400 km). But as we go higher (> 400 km) the density of the atmosphere reduces and so do the effects of differential drag.

The objective of this paper is to find the effective range of altitudes for which formation maintenance with differential drag is feasible. The study will also help to identify the necessary differential drag-area requirements for controlling a nano-satellite formation. Based on the study results, a control law is developed that adjusts the cross-sectional area of the satellites by comparing the energies of the satellites in formation. There are several other control methods in literature that treat this type of problem [7–10].

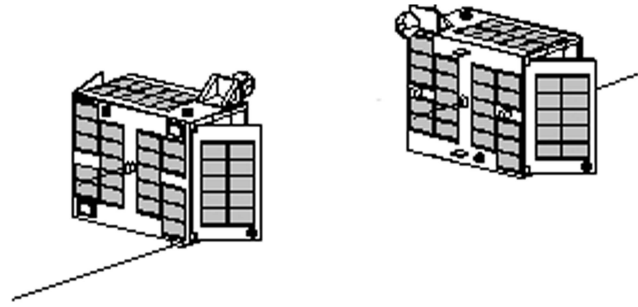


Fig. 1. Example of formation keeping with drag panels.

It should be noted that the objective of this paper is not to provide the best control method but to determine feasibility of the concept for spacecraft formation flight. The whole study was conducted with the help of the high precision orbit propagator (HPOP) module of the Satellite Tool Kit (STK) and the control laws were implemented in Matlab/Simulink. Unless stated, the atmospheric model used in the simulations was the Naval Research Laboratory Mass Spectrometer and Incoherent Scatter Radar (NRLMSISE) 2000 [11].

II. FEASIBILITY STUDY

A. Factors that Affect Differential Drag

For the feasibility study, we consider two almost identical nano-satellites weighing 8 kg flying in a leader-follower formation as shown in Fig. 1. The orbits are assumed to be circular. We assume equal effective cross-sectional areas of 0.09 m^2 ($0.3 \text{ m} \times 0.3 \text{ m}$) and drag coefficients of 2.0. The orbits of the spacecraft are considered to be Sun-synchronous. The satellites have drag panels that can open and close to a variable extent to control their relative positions. For simulation purposes, a 10% difference (0.009 m^2) in drag area is assumed. It should not be difficult to interpolate the effects for cases with more or less drag area as the differential drag acceleration is directly proportional to the difference in area. The magnitude of drifts they can achieve with differential drag depends directly on the density of the atmosphere, which in turn depends on many factors like the solar flux, the geomagnetic activity, and the operational altitude.

Solar flux, or the incident radiation arriving from the Sun, affects the atmospheric density through nearly instantaneous heating from extreme ultraviolet radiation (EUV or FEUV). Geomagnetic activity affects the atmosphere through delayed heating of atmospheric particles from collisions with charged energetic particles from the Sun. Together these effects increase the atmospheric density at higher altitudes by increasing particle collisions. The level of solar flux and geomagnetic activity at any time are difficult to predict but fall within a range of values. For the solar flux, the F10.7 (FEUV) values are

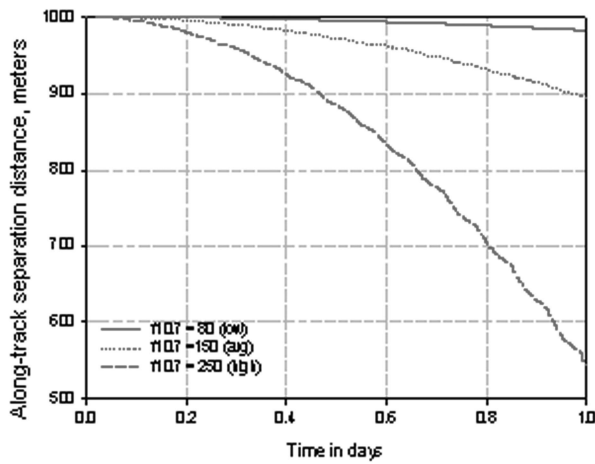


Fig. 2. Along-track drift due to a 10% differential drag-area at different solar activity periods for 600-km altitude.

between 70 to 300 SFU (1 solar flux unit or SFU = 1×10^{-22} W/m² Hz) depending on the period of solar activity [12]. The geomagnetic planetary index k_p varies from 0 (low activity) to 9 (high activity).

The drifts achievable with a 10% differential drag-area for different solar activity periods at 600-km altitude are shown in Fig. 2. In the simulations, the formation was initially spaced at 1000 m and the cross-sectional area of the deputy satellite was increased by 10%. A simulation step size of 1 s and a simulation time of 1 day yielded the following results.

At low solar activity, the drifts in the along-track direction and the radial direction due to 10% differential drag-area are almost 15 m/day and 0.15 m/day, respectively. Drag also decreases the altitude of the master spacecraft by 2 m/day for the assumed spacecraft configuration. Please note that the drift in the along-track direction is nonlinear and is provided here in drift/day format only for comparison purposes.

For normal solar activity periods, the drifts in the along-track direction and the radial direction due to 10% differential drag-area are almost 110 m/day and 1.2 m/day, respectively. The loss of altitude for such an activity period is 13 m/day.

For high solar activity period, the drifts in the along-track direction and the radial direction due to 10% differential drag-area are almost 460 m/day and 4.5 m/day, respectively. The loss of altitude of the master spacecraft for such an activity period is 57 m/day. The results of the simulation are summarized in Table I.

It can be seen from the simulation results that the drifts are significant in magnitude even at low solar activity for the 600 km altitude. This is because the drifts are caused not only by the differential drag acceleration but also by the velocity increase due to the radial drift.

The planetary geomagnetic index k_p , also changes with time and affects the differential drag acceleration

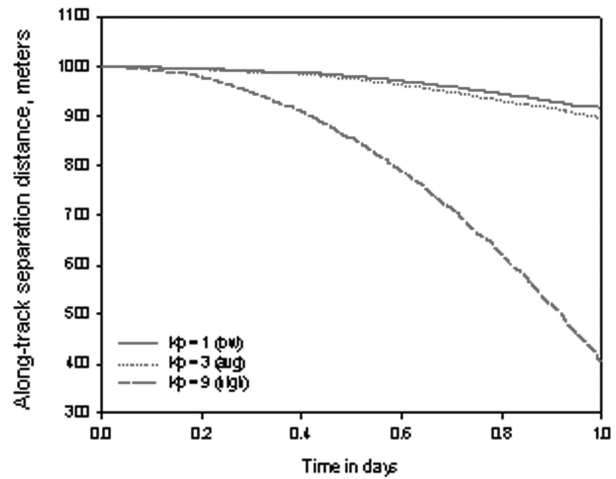


Fig. 3. Along-track drift due to a 10% differential drag at different geomagnetic activity periods for 600-km altitude.

TABLE I
Drifts Due to 10% Differential Drag-Area at Different Solar Activity Periods for 600 km Altitude

	Along-Track Drift/day	Radial Drift/day	Altitude Loss/Day
Low Solar Activity (F10.7 = 80)	15 m	0.15 m	2 m
Normal Solar Activity (F10.7 = 150)	110 m	1.2 m	13 m
High Solar Activity (F10.7 = 250)	460 m	4.5 m	57 m

values. The instantaneous value of k_p depends on many factors like sunspot cycles, solar flares, coronal holes, disappearing solar filaments and the solar-wind environment near the Earth. Rhoden [13] found that atmospheric densities increase by as much as 134% in response to an increase in the k_p index from 1 to 6.

The along-track drift achievable with a differential drag of 10% at 600 km altitude for different k_p is shown in Fig. 3. The simulations were performed for normal solar activity period (F10.7 = 150). It can be seen that the drift values are 10 times more for high geomagnetic activity than when compared with the drift at normal activity. Even for low values of k_p , the drift in the along-track direction is approximately 60 m/day for a 10% differential drag-area.

The operation altitude is also one of the main factors that affect the differential drag acceleration values. Fig. 4 illustrates the drifts achievable with a 10% differential drag-area at solar minima for different operation altitudes. The same results are summarized in Table II.

It can be seen from Table II that the drift due to differential drag decreases with the increasing altitude.

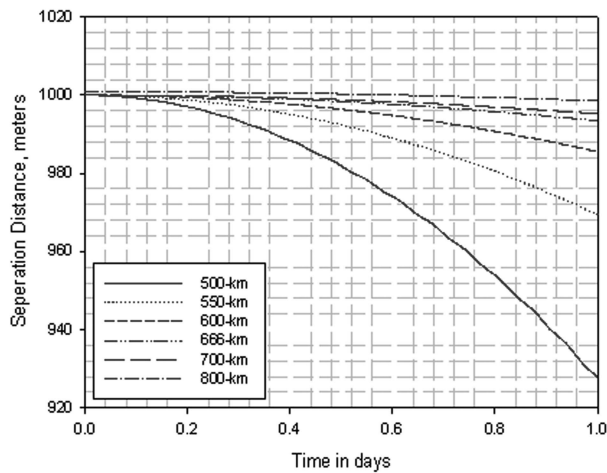


Fig. 4. Drift achievable with a 10% differential drag-area for various altitudes at low solar activity.

TABLE II

Drift Values Achievable with 10% Differential Drag-Area for Various Altitudes at Low Solar Activity

	500 km	550 km	600 km	650 km	700 km	800 km
Drift, m/day	75	30	15	6.75	4.5	2.4

For 600 km altitude, 50% more differential drag-area is needed to produce the same drift as at 500 km. For 800 km altitude, this value rises to 300%. It should be noted that the values of the drifts are for the worst case scenario calculated using the NRLMSISE model which is estimated to have an uncertainty of 30% [14].

To assess the performance of the density model used (NRLMSISE), the values of drifts obtained at average solar flux were compared with those obtained with the other density models like Jacchia 1971, CIRA 1972, Harris-Priester, and the 1976 Standard. The results (Fig. 5) show that the NRLMSISE, Jacchia 1971, and CIRA 1972 yield almost similar results but 1976 Standard and the Harris-Priester show some significant deviations. Comparing atmospheric models is difficult for a variety of reasons: there is usually no direct measurement of density, only the indirect measure from the satellite motion which involves additional unknowns; models vary in their accuracy over regions of the atmosphere and solar conditions, leading to mixed results. However, Harris-Priester and the 1976 Standard models are known to be not precise and NRLMSISE and Jacchia models are known to be better models for density prediction [15].

The value of differential drag acceleration produced by 0.01 m^2 of drag-area for different altitudes at different solar activity periods is shown in Fig. 6. The drag acceleration values range from $5.8 \times 10^{-9} \text{ m/s}^2$ for 500-km altitude to $1.8 \times 10^{-10} \text{ m/s}^2$ for 800-km altitude at low solar activity, $3.8 \times 10^{-8} \text{ m/s}^2$

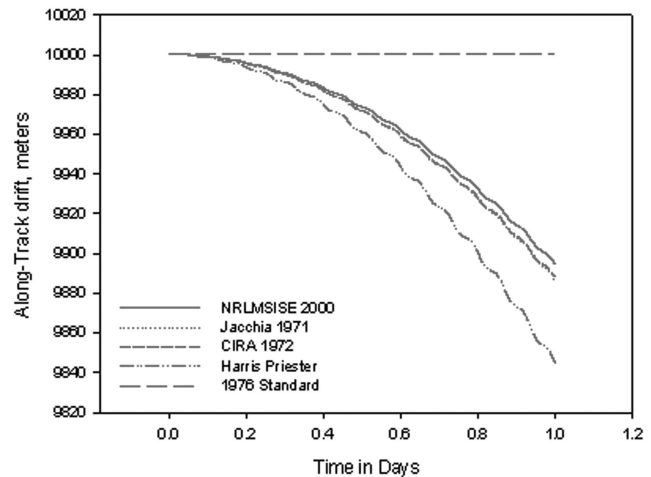


Fig. 5. Drift values obtained from different atmospheric density models.

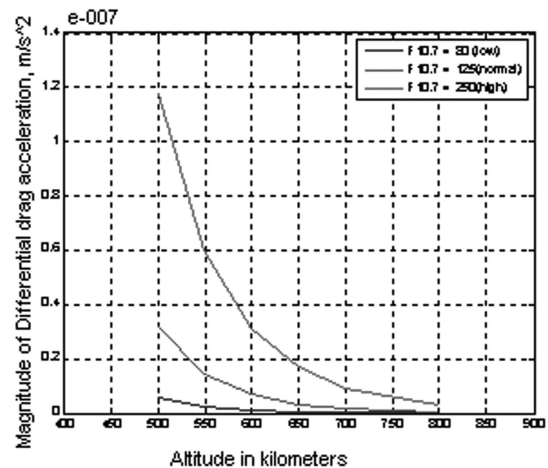


Fig. 6. Differential drag acceleration produced by 0.01 m^2 drag area for different altitudes as different solar activity periods.

for 500-km altitude to $6.0 \times 10^{-10} \text{ m/s}^2$ for 800-km altitude at normal solar activity and $1.2 \times 10^{-7} \text{ m/s}^2$ for 500-km altitude to $2.7 \times 10^{-9} \text{ m/s}^2$ for 800-km altitude at high solar activity.

It is evident from the simulation results that a reasonable amount of drift could be achieved with the differential drag panels even at high altitudes. However, this study will not be complete without the assessment of the drifts caused by other perturbations that need to be compensated with differential drag. For this reason, the other factors that affect the formation are examined in the next section.

B. Factors that Disrupt the Formation

One of the main factors that affects a formation pattern is the differential gravitational effect [16]. The differential gravitational effects are caused due to the spacecraft passing different regions of the Earth at a given time. This causes the spacecraft to experience gravitational accelerations of different magnitudes based on the subsatellite point location. The effect

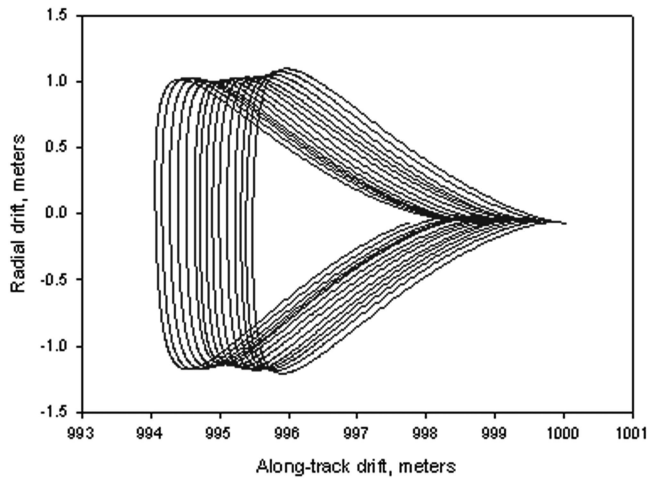


Fig. 7. Effects of differential gravity on spacecraft formation of 1 km at 600-km altitude.

can be attributed to the Earth's oblateness. To study the effects of differential gravitational acceleration, simulations were performed for a formation (at 600-km altitude) initially separated by 1 km and in Sun-synchronous orbits. The EGM-96 (Earth gravity model) model with an order and degree of 70×70 was used for the simulations. The along-track separation distance versus radial separation distance, plotted for 1 day (~ 15 orbits), is shown in Fig. 7.

It can be seen that the along-track and the radial distances oscillate within one orbit. The magnitude of these oscillations varies from 4.5 m/orbit in the along-track direction to slightly more than a meter/orbit in the radial direction. There is also a slight secular drift in the along-track direction due to the change of the argument of perigees of the orbits of spacecraft in formation. However, the mean average drift in the radial direction is zero. The magnitudes of secular drift and periodic variations were found to decrease with the decrease in the separation of the initial separation distances. For very close formations, the effects of differential J_2 are in centimeter level. Differential gravitational affects also cause drifts in the cross-track direction. These drifts become significant if the spacecrafts lie in different orbital planes or have different semi-major axis.

Navigation errors lead to uncertainty of position and velocity at any given time. These uncertainties would usually be considered as drifts by the control system. Carpenter [17] estimates that even with a navigation system that can produce radial accuracy of 10 cm and speed accuracy of 0.1 mm/s, the corresponding uncertainties of along-track drift may be on the order of 1 m/orbit, and could be as poor as about 3 m/orbit depending on the navigation filter. Although navigation errors do not disrupt the formation directly, they cause errors in the formation geometry by causing a need for unnecessary maneuvers.

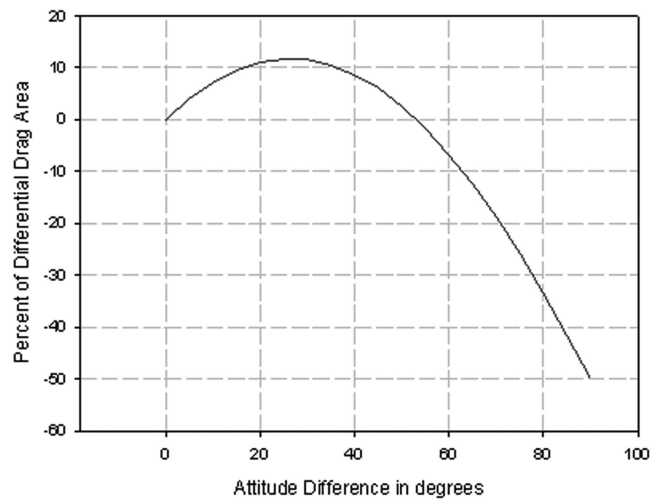


Fig. 8. Dependence of differential drag on the attitude errors.

Relative attitude errors could also affect the formation by inducing differential drag effects. The magnitude of the drifts depends directly on the percentage of differential drag induced. Let us consider an attitude control system with a control accuracy of $\pm 5^\circ$ in the three rotational directions. Generally, for identical spacecraft, a pure roll error will not contribute to any differential drag effects but pitch or yaw errors will cause differences in effective cross-sectional areas. Fig. 8 shows the percent of differential drag induced by relative attitude errors for a spacecraft configuration ($0.3 \text{ m} \times 0.3 \text{ m} \times 0.15 \text{ m}$) as shown in Fig. 1.

It can be seen from Fig. 8 that a constant 5% attitude error translates to roughly 4% differential drag-area. A 4% differential drag-area would in turn cause a drift of approximately 6 m/day in the along-track direction and 0.06 m/day in the radial direction (Table I) at low solar activity or 182 m/day in the along-track direction and 1.8 m/day in the radial direction at high solar activity. It should be noted that the plot in Fig. 8 is for a particular configuration of the spacecraft and the results might vary for different spacecraft configurations. Relative attitude errors should also be considered during operation of the drag panels to minimize control errors.

Other factors that disrupt the formation are the differential perturbations of the Sun and the Moon and the differential solar radiation pressure effects. Both of these factors only cause periodic variations in the along-track and radial separation distances that vary with the separation distance and do not cause any secular drifts for identical spacecraft. The effects of the Sun, Moon, and the solar radiation pressure along with the individual and combined effects of differential drag and differential gravity are shown in Figs. 9–11. It can be seen that the differential effects of Sun, Moon, and the solar radiation pressure are much smaller than the effects of differential drag

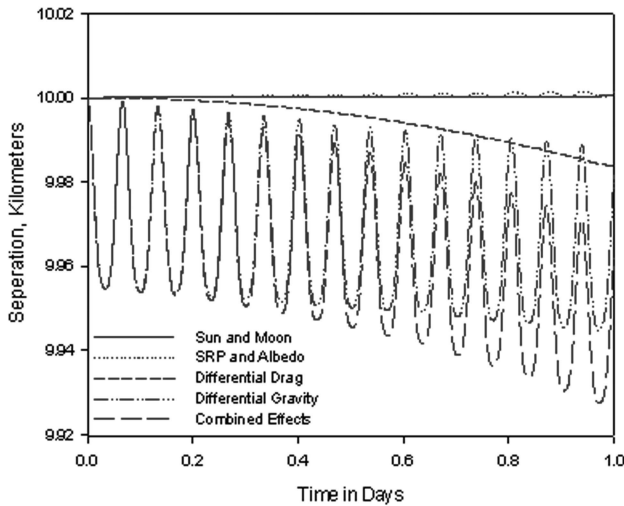


Fig. 9. Effects of differential accelerations on leader-follower formation at 600-km altitude separated by 10 km.

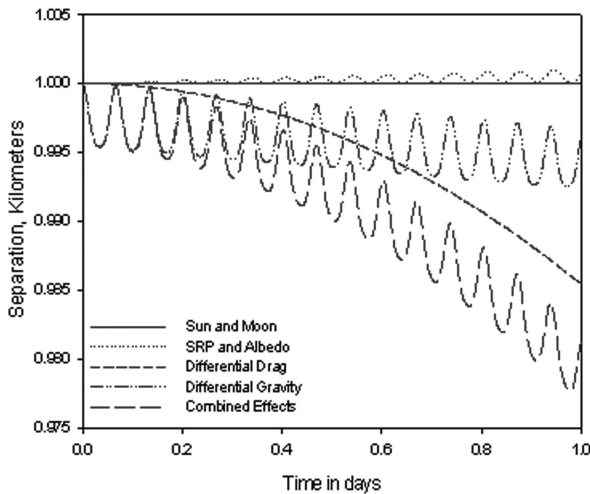


Fig. 10. Effects of differential accelerations on leader-follower formation at 600-km altitude separated by 1 km.

(10%) and differential gravity. Also the differential gravitational effects decrease with the decrease in the initial separation. This is not true for the differential drag effects, which are not dependent on the initial separation distance. For close formations, differential drag is the only major cause of satellite drift. The “Combined Effects” plot shows the drift resulting from the effects of all the factors for three different separation distances namely, 10 km, 1 km, and 100 m, respectively. It is also plotted for the worst case scenario where the drifts due to differential gravity and drag are in the same direction.

C. Conclusions of the Feasibility Study

The amount of differential drag acceleration achievable is mainly dependant on the operating altitude of the formation, the F10.7 solar flux value, the geomagnetic planetary index, and the differences in the effective cross-sectional areas. While it is

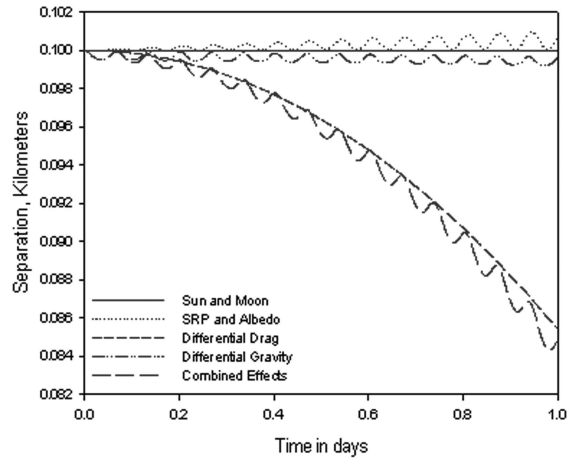


Fig. 11. Effects of differential accelerations on leader-follower formation at 600-km altitude separated by 100 m.

desirable to do any formation flying demonstration at altitudes lower than 400 km, it is possible to achieve enough drifts to compensate for the disturbing perturbations even at 800-km altitude with large drag area differences. Whether this is achievable with small nano-satellites becomes a questionable issue due to the limited drag surface area available. Another important factor that dictates controllability with differential drag is the separation distance. The differential gravitational effects seem to increase in magnitude with the increasing separation distances. For a given satellite configuration, with a given effective differential drag-area and for a given altitude there will be a break-off separation distance that will limit effective controllability of a formation. Any larger than the break-off distance, the formation will become uncontrollable. While it is not difficult to calculate the break-off distance, this paper does not include such a calculation due to the numerous numbers of variables and scenarios involved.

It is very important to stop the drift of the spacecraft after inter-satellite separation. The time taken to stop the drift will definitely dictate the initial separation distance and that depends on the magnitude of differential drag acceleration. One good way to reduce the impact of an initial velocity on along-track growth rate is by separating the satellites in the radial or the cross-track direction. The resultant cross-track drift is not controllable though. A collision scenario is possible if separation occurs in a plane perpendicular to the velocity direction and hence that direction should be avoided.

III. PID CONTROLLER FOR FORMATION KEEPING

In this section, the design of a simple PID controller for formation keeping is discussed. The controller takes into account the difference of energies of the orbits of the spacecraft and assigns a control drag-area δA to nullify the difference according to the

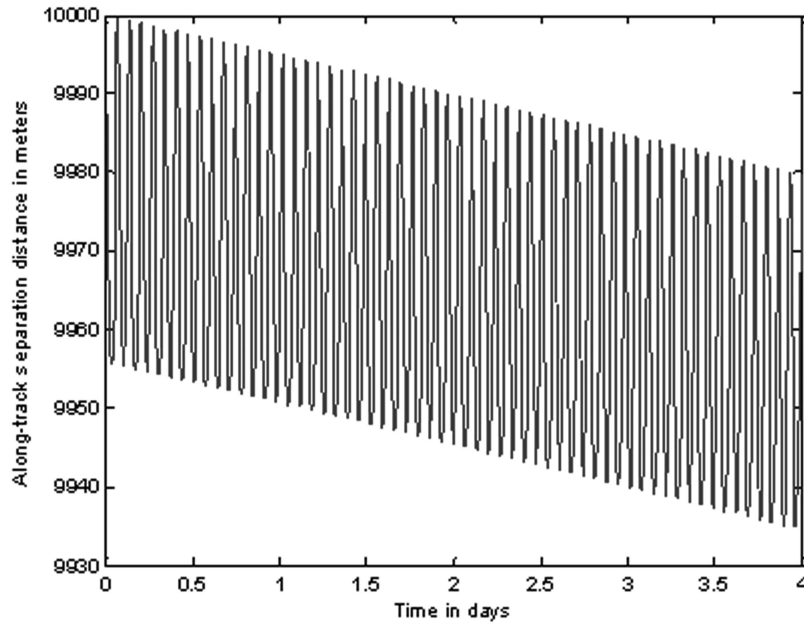


Fig. 12. Evolution of along-track distance without active control.

control law;

$$\delta A = K_p \cdot \delta E + K_I \cdot \int \delta E dt + K_d \cdot \frac{d\delta E}{dt} \quad (2)$$

where

$$\delta E = E_m - E_d = \frac{V_m^2}{2} - \frac{\mu}{R_d} - \left(\frac{V_d^2}{2} - \frac{\mu}{R_d} \right).$$

Subscripts m and d correspond to master and deputy spacecraft, respectively.

The control drag-area may be assigned to either the master spacecraft or the deputy spacecraft depending on the sign of the difference of δE . The control drag-area is used to compute the control acceleration that is given by

$$a_{\text{control}} = -\frac{\rho}{2} \left(\frac{C_d \cdot (A + \delta A)}{m} \right) V_{\text{rel}}^2 \frac{\vec{V}_{\text{rel}}}{|\vec{V}_{\text{rel}}|}. \quad (3)$$

The control acceleration is then used by the system equation that is given as

$$\ddot{\vec{r}} = -\frac{\mu}{r^3} \hat{r} + a_{\text{control}} + a_{\text{perturbations}}. \quad (4)$$

The term in (4) may include the effects of accelerations that cause the drift of the formation including that of the differential gravity and the differential drag effects caused by attitude errors.

In a real mission scenario, the orbital energies of the master and deputy spacecraft would be calculated using the position and velocity feedback from the on-board GPS receivers. Since these data represent single point measurements, there is no need for any relative navigation system to implement this controller.

To test the functionality of the controller, simulations involving formation maintenance were performed in a high-fidelity environment with the

inclusion of Earth oblateness effects, Sun and Moon perturbations, and solar radiation pressure. The satellites were assumed to have an initial along-track separation distance of 10 km. The controller's gains were selected based on the observed energy differences in the free runs. A saturation function was implemented to limit the drag area differences to a maximum of 0.01 m². A control value of $+u$ meant that the master spacecraft would change its drag area and a control value of $-u$ meant that the follower would change its drag area. The following controller gains were found to produce reasonable results; $K_p = 10^5$, $K_i = 200$, and $K_d = 3 \times 10^3$ although a finer tuning could have yielded even better results.

The relative motion of the deputy spacecraft with respect to the master spacecraft, in the along-track and radial directions without active control (propagated for 4 days) is shown in Figs. 12 and 13. The relative motion in the along-track direction is the same as in Fig. 9 only without any differential drag.

The simulations were performed again but this time with the PID controller switched on. Figs. 14 and 15 show the controlled along-track and radial separation distances. The controller managed to cancel the along-track drift and also reduce periodic oscillations in the along-track and radial directions. The along-track separation distance remained at 10 km for the simulated time. The control switch values are shown in Fig. 16. For the selected gains, the system operates at saturation. An increase in the magnitude of the gain made the system work within saturation but also increased the transient time. Proper tuning of the gains could lead to better results in terms of transient time and steady state errors.

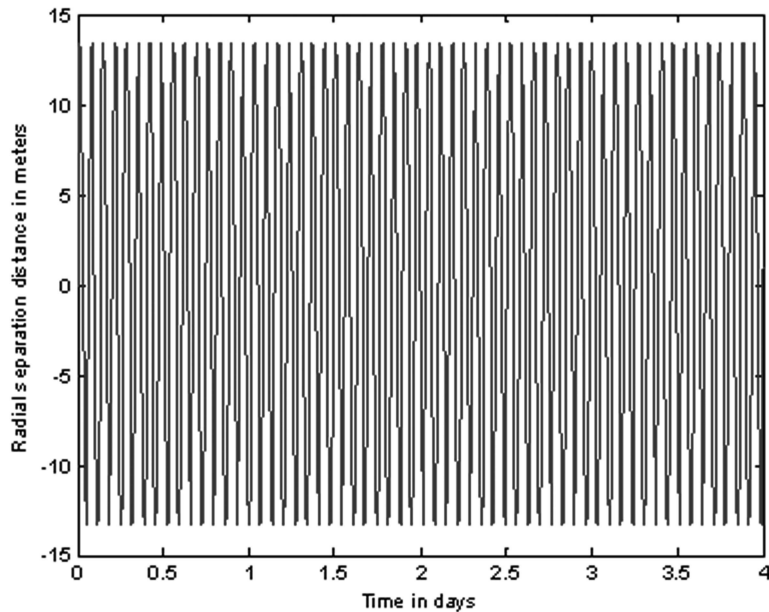


Fig. 13. Evolution of radial distance without active control.

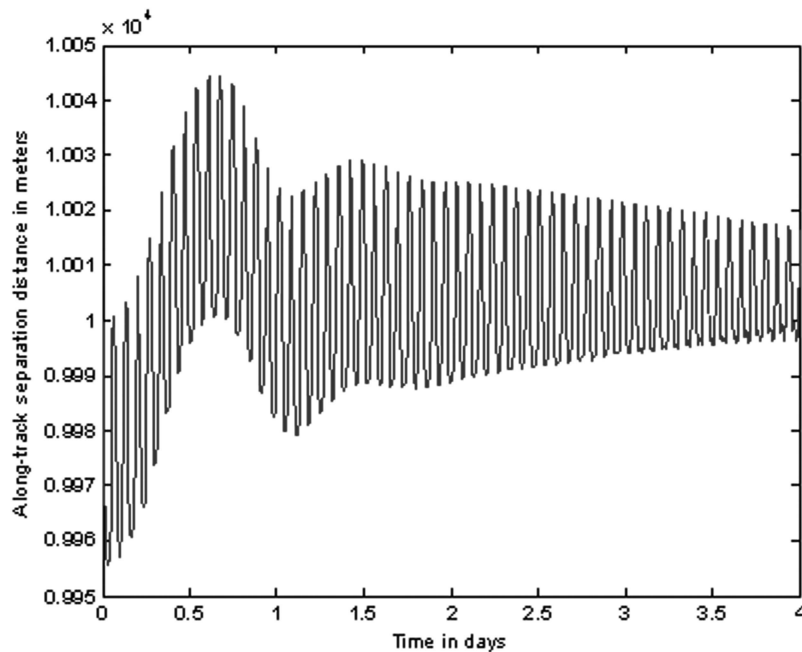


Fig. 14. Evolution of along-track distance with active control.

From the simulation results, it can be seen that the controller works reasonably well for small differences in energy caused by natural perturbations. The advantage of the controller proposed in this paper is its ease of implementation and moderate requirements for formation keeping. It is reasonable to believe that the controller would not be able to compensate the errors caused by huge radial separation distances or significant velocity offsets caused after spacecraft deployment. For these cases, a conventional propulsion system would be more appropriate as a drag controller would demand huge cross-sectional areas to nullify the energy

difference. There are some issues that have not been addressed here and currently being investigated. They are:

- 1) robustness of the controller to feedback errors,
- 2) dependence of the stability of the controller on initial conditions/parameters.

Currently, at the time of writing this paper, the authors are investigating other control methods of formation keeping and reconfiguration using differential drag. The results reported in this paper are excerpts of a feasibility study conducted for a proposed formation flight mission of the Canadian

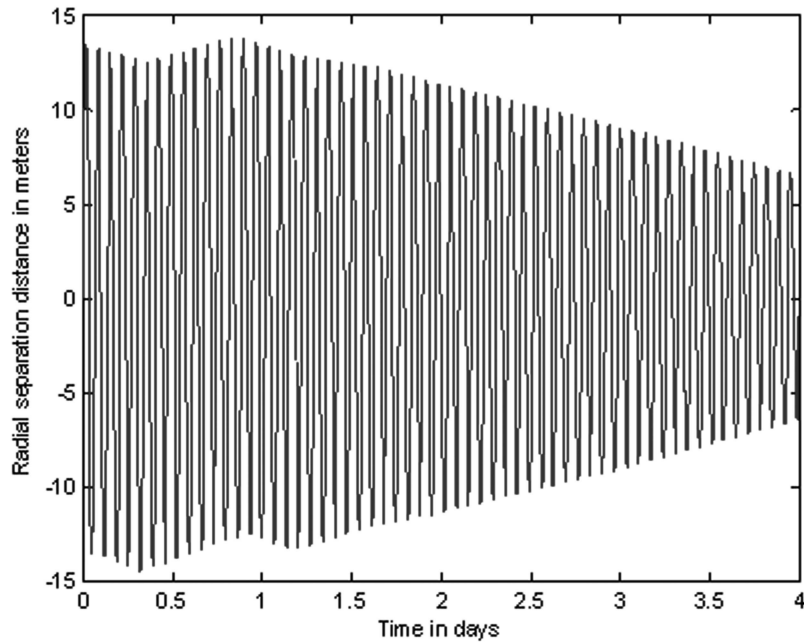


Fig. 15. Evolution of radial distance with active control.

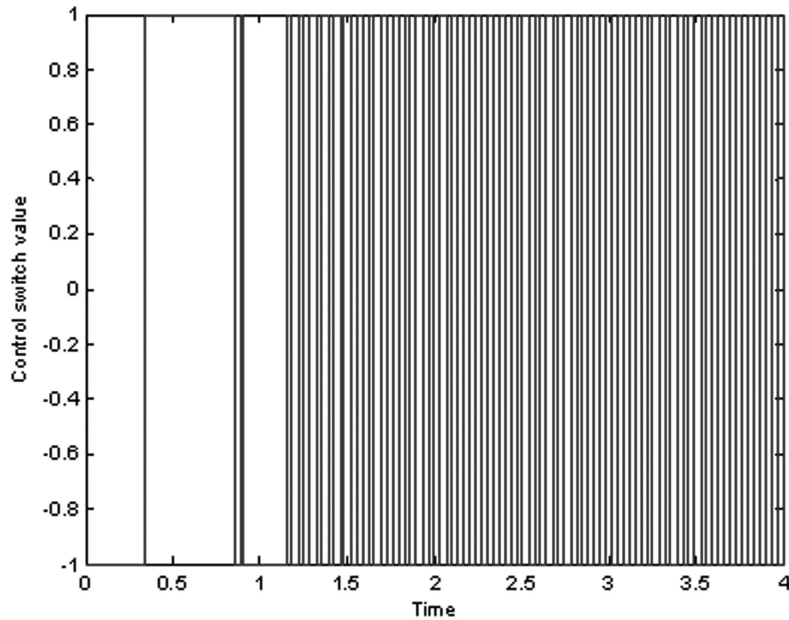


Fig. 16. Control switch values used for formation maintenance.

Space Agency that is scheduled to be launched in 2011.

IV. SUMMARY

This paper addresses the feasibility of using differential drag for formation keeping of a leader-follower formation in circular orbits by comparing the drifts achievable with differential drag at different solar activity periods to the drifts caused by various other factors like the differential gravitational and navigation errors. The simulations performed with the HPOP module of the STK showed that it is possible to achieve enough drift

to compensate the drifts produced by differential gravitational and other differential effects even at low solar activity period with a moderate differential drag-area for altitudes 500 km–800 km. A control law was also developed for formation keeping that adjusts the cross-sectional area of the satellites by comparing the energies of the satellites in formation. The simulations performed in a high fidelity environment using an in-house built propagator showed that the controller could maintain the formation distance with coarse control accuracy of a few tens of meters and simultaneously reduce any periodic oscillations in the in-track-radial plane.

REFERENCES

- [1] Leonard, C. L.
Orbital formation-keeping with differential drag.
Journal of Guidance, Control, and Dynamics, **12**, 1 (1989), 108–113.
- [2] King, L. B., Parker, G. G., Deshmukh, S., and Chong, J.
Spacecraft formation-flying using inter-vehicle Coulomb forces.
NIAC Phase I Final Report, 2002. Available: http://www.niac.usra.edu/files/studies/final_report/601King.pdf
- [3] Kong, E. M., Kwon, D. W., Schweighart, S. A., Elias, L. M., Sedwick, R. J., and Miller, D. W.
Electromagnetic formation flight for multisatellite arrays.
AIAA Journal of Spacecraft and Rockets, **41**, 4 (2004), 659–666.
- [4] Bae, Y. K.
A contamination-free ultrahigh precision formation flying method for micro, nano, and pico-satellites with nanometer accuracy.
Available: http://www.baeminstitute.com/downloads/STAIF_2006_YK_Bae_FF_Paper.pdf
- [5] Maclay, T. and Tuttle, C.
Satellite stationkeeping of the ORBCOMM constellation via active control of atmospheric drag: Operations, constraints, and performance.
Advances in the Astronautical Sciences, **120**, Part I, 763–773.
- [6] Vallado, D.
Fundamentals of Astrodynamics and Applications (2nd ed.).
New York: Springer, 2001, 522–523.
- [7] Palmerini, G. B., Sgubini, S., and Taini, G.
Spacecraft Orbit Control using Air Drag.
Paper IAC-05-c1.6.10, 2005.
- [8] Mathews, M. and Leszkiewicz, S.
Efficient Spacecraft Formationkeeping with Consideration of Ballistic Control.
AIAA AA-88-0375, Jan. 1988.
- [9] Gurfil, P. and Kasdin, N. J.
Nonlinear low-thrust Lyapunov-based control of spacecraft formations.
In *Proceedings of the American Control Conference*, Denver, CO, June 4–6, 2003, 1758–1763.
- [10] Starin, S., Scott, R., Yedavalli, R. K., and Sparks, A.
Design of a LQR controller of reduced inputs for multiple spacecraft formation flying.
In *Proceedings of the American Control Conference*, June 25–27, 2001, 118–126.
- [11] Picone, J. M., Hedin, A. E., Drob, D. P., and Aikin, A. C.
NRLMSISE-00 empirical model of the atmosphere: Statistical comparisons and scientific issues.
Journal of Geophysical Research, **107**, A12 (2002).
- [12] Schatten, K. H.
Solar activity and the solar cycle.
Advances in Space Research, **32**, 4 (Aug. 2003), 451–460.
- [13] Rhoden, E. A., Forbes, J. M., and Marcos, F. A.
The influence of geomagnetic and solar variabilities on lower thermosphere density.
Journal of Atmospheric and Terrestrial Physics, **62** (2000), 999–1013.
- [14] Part, J., et al.
Comparison between the KOMPSAT-1 drag derived density and the MSISE model density during strong solar and/or geomagnetic activities.
Earth Planets Space, **60** (2008), 601–606.
- [15] Akins, K., Healy, L., Coffey, S., and Picone, M.
Comparison of MSIS and Jacchia Atmospheric Density Models for Orbit Determination and Propagation.
Paper AAS 03-165, 2003.
- [16] Balaji, S. K. and Tatnall, A.
System design issues of small formation-flying spacecraft.
In *Proceedings of the IEEE Aerospace Conference*, 2003, 2587–2597.
- [17] Carpenter, J. R. and Alfriend, K. T.
Navigation accuracy guidelines for orbital formation flying.
Journal of the Astronautical Sciences, **53**, 2 (2005), 207–219.
- [18] Sabatini, M. and Palmerini, G. B.
Linearized formation-flying dynamics in a perturbed orbital environment.
In *Proceedings of the IEEE/AIAA Aerospace Conference*, Mar. 1–8, 2008, 1–13.

Balaji Shankar Kumar graduated from the University of Southampton, England in 2005 with a Ph.D. in astronautics.

From 2006 to 2009, he was a visiting research scientist at the Canadian Space Agency. He is currently working as a space missions analyst at COMDEV Ltd. in Cambridge, Canada. His field of expertise is astrodynamics and spacecraft engineering. He has previously worked for the Indian Space Research Organization as a spacecraft systems engineer and for the Russian Space Agency as a Student Trainee.

Alfred Ng received his Ph.D. in mechanical engineering in 1992 from University of British Columbia, Canada.

Shortly after graduation, he joined the Canadian Space Agency as a research scientist, Orbital and Attitude Dynamics and Control. Currently he is a manager of the Control and Analysis Group in the Directorate of Spacecraft Engineering, responsible for internal and external R&D in the areas of active shape control, attitude determination and control systems, formation flying of multiple spacecraft, and orbit analysis and control.

Keisuke Yoshihara received the B.S. and M.S. degree in mechanical engineering from Tokyo Institute of Technology, Tokyo, Japan, in 1998 and 2000, respectively.

He had been a research engineer of the Space Technology Demonstration Research Center of the Japan Aerospace Exploration Agency (JAXA). He joined in several microsatellite projects such as the Micro-LabSat and JC2Sat.

Mr. Yoshihara is a member of The Japan Society of Mechanical Engineers.

Anton de Ruiter received a B.E. degree in mechanical engineering from the University of Canterbury in 1999, and an M.A.Sc. and Ph.D. in aerospace engineering from the University of Toronto in 2001 and 2005, respectively.

From 2006 to 2008 he was a visiting research scientist at the Canadian Space Agency. He is currently an assistant professor at Carleton University in Ottawa, Canada. His areas of expertise include control systems design, state estimation, and inertial navigation systems. His research interests include integrated GPS/INS navigation, spacecraft formation flying, spacecraft attitude control, and multiple objective control design for decentralized systems.